Clinical Cancer Research

Purinostat Mesylate Is a Uniquely Potent and Selective Inhibitor of HDACs for the Treatment of *BCR-ABL*–Induced B-Cell Acute Lymphoblastic Leukemia

Linyu Yang[1], Qiang Qiu[1], Minghai Tang[1], Fang Wang[1], Yuyao Yi[2], Dongni Yi[2], Zhuang Yang[1], Zejiang Zhu[1], Shoujun Zheng[1], Jianhong Yang[1], Heying Pei[1], Li Zheng[1], Yong Chen[1], Liping Gou[1], Liya Luo[1], Xing Deng[1], Haoyu Ye[1], Yiguo Hu[1], Ting Niu[1,2], and Lijuan Chen[1]

Abstract

Purpose: This study was to perform preclinical evaluation of a novel class I and IIb HDAC-selective inhibitor, purinostat mesylate, for the treatment of Ph^+ B-cell acute lymphoblastic leukemia (B-ALL).

Experimental Design: Biochemical assays were used to test enzymatic activity inhibition of purinostat mesylate. Ph^+ leukemic cell lines and patient cells were used to evaluate purinostat mesylate activity *in vitro*. BL-2 secondary transplantation Ph^+ B-ALL mouse model was used to validate its efficacy, mechanism, and pharmacokinetics properties *in vivo*. *BCR-ABL(T315I)*–induced primary B-ALL mouse model and PDX mouse model derived from relapsed Ph^+ B-ALL patient post TKI treatment were used to determine the antitumor effect of purinostat mesylate for refractory or relapsed Ph^+ B-ALL. Long-term toxicity and hERG blockade assays were used to safety evaluation of purinostat mesylate.

Results: Purinostat mesylate, a class I and IIb HDAC highly selective inhibitor, exhibited robust antitumor activity in hematologic cancers. Purinostat mesylate at low nanomolar concentration induced apoptosis, and downregulated BCR-ABL and c-MYC expression in Ph^+ leukemia cell lines and primary Ph^+ B-ALL cells from relapsed patients. Purinostat mesylate efficiently attenuated Ph^+ B-ALL progression and significantly prolonged the survival both in BL-2 secondary transplantation model with clinical patient symptoms of Ph^+ B-ALL, *BCR-ABL(T315I)*–induced primary B-ALL mouse model, and PDX model derived from patients with relapsed Ph^+ B-ALL post TKI treatment. In addition, purinostat mesylate possesses favorable pharmacokinetics and low toxicity properties.

Conclusions: Purinostat mesylate provides a new therapeutic strategy for patients with Ph^+ B-ALL, including those who relapse after TKI treatment.

Introduction

Philadelphia chromosome–positive (Ph^+) leukemia is a common hematologic malignancy, which is characterized by Philadelphia chromosome. Ph chromosome is a specific genetic abnormality resulting in chromosome translation of t (9;22) (q34; q11.2), which forms a chimeric and constitutively activated BCR-ABL tyrosine kinase (1, 2). Approximately 95% of patients with chronic myeloid leukemia (CML) and 20% of B-cell acute lymphoblastic leukemia (B-ALL) patients carry the BCR-ABL (3). Although BCR-ABL–specific tyrosine kinase inhibitors (TKI; such as imatinib, nilotinib, and dasatinib) have achieved significantly improvement in the treatment of CML and Ph^+ B-ALL (4–6), TKI resistance due to the mutation of *BCR-ABL* still occurs in a certain portion of patients with CML and B-ALL (7, 8). Among them, T315I mutation is more susceptible to TKI resistance (9–11). Despite the third-generation TKI ponatinib has the unique property of inhibiting BCR-ABL(T315I) mutation (12, 13), responses in patients with CML in the blastic phase (CML-BP) or Ph^+ B-ALL are typically transient (14, 15). Recently, the FDA-approved tisagenlecleucel and axicabtagene ciloleucel chimeric antigen receptor T cells (CAR-T) therapies significantly improved the therapy efficacy of B-ALL via the immunotherapies directed against the CD19 (16–18). However, the escape mechanisms are common (19). An unintentional introduction of a single leukemia B cell during T-cell production could result in resistance to CAR-T therapy (20). For these reasons, there is an urgent need to develop new therapeutic drugs for the treatment of Ph^+ B-ALL.

Epigenetic drugs that target histone deacetylase (HDAC) enzymes have been proven successful in the treatment of hematologic malignancies (21–25). HDAC inhibitors inhibit deacetylation of lysines in histones and nonhistone cellular proteins, inducing hyperacetylation and opening chromatin conformation (22). HDAC inhibitors exert anticancer activity by altering

[1]State Key Laboratory of Biotherapy and Cancer Center, National Clinical Research Center for Geriatrics, West China Hospital of Sichuan University, Chengdu, China. [2]Department of Hematology and Research Laboratory of Hematology, West China Hospital of Sichuan University, Chengdu, China.

Note: Supplementary data for this article are available at Clinical Cancer Research Online (http://clincancerres.aacrjournals.org/).

L. Yang, Q. Qiu, and M. Tang contributed equally to this article.

Corresponding Authors: Lijuan Chen, West China Hospital, Sichuan University, Chengdu, Sichuan 610041, China. Phone: 8628-8516-4063; Fax: 8628-8516-4060; E-mail: chenlijuan125@163.com; Ting Niu, tingniu@sina.com; and Yiguo Hu, huyiguo@scu.edu.cn

Clin Cancer Res 2019;25:7527–39

doi: 10.1158/1078-0432.CCR-19-0516

Translational Relevance

Here, we report a novel class I and IIb HDAC-selective inhibitor, purinostat mesylate, which exhibited superior efficiency against Ph^+ B-cell acute lymphoblastic leukemia (B-ALL) both *in vitro* and *in vivo*. At nanomolar or sub-nanomolar concentration, purinostat mesylate induced Ph^+ cell apoptosis and altered the expression of some key proteins such as BCR-ABL and c-MYC in cell lines of BL-2, LAMA84, and primary cells isolated from patients with B-ALL relapsed. Purinostat mesylate significantly prolonged the survival of mice that received secondary transplanted BL-2 cells, *BCR-ABL (T315I)*–induced primary B-ALL cells, or Ph^+ B-ALL cells from relapsed patient with TKI treatment, respectively. In addition, purinostat mesylate possesses favorable pharmacokinetics and low toxicity properties. Currently, purinostat mesylate has been approved by the National Medical Products Administration (NMPA) of China for clinical trials for the treatment of relapsed or refractory B-cell–associated hematologic malignancies. Collectively, our data provide preclinical bases for clinical trials of purinostat mesylate in patients with Ph^+ B-ALL including those who relapse post TKI treatment.

gene transcription, inducing cell growth arrest, apoptosis, and inhibiting tumor angiogenesis. Several studies have shown that heat shock protein 90 (HSP90) was a critical target of HDAC inhibitors in B-cell lymphoma cells (26). HDAC inhibitors caused HSP90 to lose its chaperone function and expose its client protein such as BCR-ABL to polyubiquitination (24). In addition, BCR-ABL activates multiple signaling pathways including c-MYC (27) and SRC kinases (28, 29). Therefore, downregulation of c-MYC and SRC kinases is important for the treatment of Ph^+ B-ALL. To date, five HDAC inhibitors (vorinostat, romidepsin, belinostat, panobinostat, and chidamide) have been approved for clinical cancer treatment (30–33). Among them, panobinostat (LBH589) has been reported the most active and had been approved for multiple myeloma treatment in 2015 (34). The other four agents have been approved for T-cell lymphoma (23, 33, 35, 36). Except for chidamide as a class I HDAC- and HDAC10 subtype–selective inhibitor, romidepsin as a HDAC1- and HDAC2-selective inhibitor (33), the other three are pan-HDAC inhibitors (23). Several studies have shown that inhibition of HDAC IIa and IV enzymes had more side effects (37–39). For example, panobinostat has a boxed warning in "Highlights of prescribing information" due to severe diarrhea occurring in 25% of LBH589-treated patients, severe and fatal cardiac ischemic events, severe arrhythmias, and ECG changes (40). Therefore, it is particularly important to develop novel selective subtype HDAC inhibitors that have better efficacy and lower toxic side effects.

In a previous study, our group reported a new highly potent first-in-class HDAC inhibitor named purinostat, with significant antitumor capability of solid and hematologic tumors, such as HCT116, MV4-11, Ramos, and MM1S xenograft models (41). Here, the main objective of this study was to perform comprehensive preclinical evaluation of purinostat mesylate for Ph^+ B-ALL treatment. Purinostat mesylate was designed as a potent class I and IIb HDAC-selective inhibitor. We verified the significant antitumor ability of purinostat mesylate *in vivo* by using a highly malignant BL-2 secondary transplantation mouse model with clinical patient symptoms of Ph^+ B-ALL. More importantly, purinostat mesylate significantly extended the survival both in *BCR-ABL(T315I)*–induced B-ALL mouse model and patient-derived tumor xenograft (PDX) Ph^+ B-ALL model derived from relapsed patient post TKI treatment. The promising pharmacokinetic properties and low toxicity also supported that purinostat mesylate was a potential agent for the clinical treatment of patients with Ph^+ B-ALL including those who relapse post TKI treatment.

Materials and Methods

Compounds

Purinostat mesylate was synthesized in our laboratory (41). The purity and dissolution method for *in vitro* and *in vivo* studies were described in Supplementary Methods. LBH589 lactate was purchased from Shanghai Qibei Pharmaceutical Technology Co., Ltd., batch number 170702, purity 98.2%. D_3-purinostat mesylate was synthesized in Chengdu Maijing Biomedical Co., Ltd. with 98.33% content.

Cell culture

Cell lines MV4-11, MOLM-13, LAMA84, K562, RPMI-8226, MM1s, OCI-LY1, SUDHL-4, and Jeko-1 were obtained from ATCC. Raji and Ramos were obtained from Cell Resource Center, Shanghai Institutes for Biological Sciences, Chinese Academy of Sciences (Beijing, China). All the cells were tested and authenticated in 2017 as described previously (42). All cell lines were cultured in RPMI1640 medium supplemented with 10% FBS (Gibco) and 100 U/mL penicillin/streptomycin (Gibco) at 37°C in a humidified incubator with 5% CO_2.

BCR-ABL–positive B-ALL patient samples

Primary B-ALL patient cells with *BCR-ABL* or *BCR-ABL(T315I)* mutation were obtained from West China Hospital and approved by West China Hospital of Sichuan University (Chengdu, China) clinical ethics committee (clinical information is summarized in Supplementary Fig. S2H).

Animal experiments

All animal studies were performed in accordance with the guidelines approved by the Institutional Animal Care and Use Committees of Sichuan University (Chengdu, China).

BL-2 cell was isolated from pleural effusion of BCR-ABL–induced B-ALL mouse. The isolated and cultured methods were described in a previous study (29). The BL-2 secondary transplantation mouse model was generated by intravenous inoculation of 1×10^6 BL-2 cells into 7- to 8-week-old female C57BL/6 mice.

For the *BCR-ABL(T315I)*–induced B-ALL mouse model, the retroviral vector MSCV-IRES-GFP carrying *BCR-ABL(T315I)* cDNA, retroviral transduction, and transplantation of mouse bone marrow (BM) cells for induction of ALL by *BCR-ABL* were developed as described previously (2, 29). Seven- to 8-week-old female recipient mice C57BL/6 were prepared by 1,100 cGy gamma irradiation and 1.0×10^6 donor cells were transplanted via tail vein.

The patient-derived xenograft (PDX) model was established with primary cells isolated from Ph^+ B-ALL relapsed patient post TKI treatment (patient #2). This patient sample with *IKZF1* deletion involving exons 4–7 was identified by PCR (forward

primer: ATGGATGCTGATGAGGGTCAAGAC, reverse primer: CCACGTGATGGACCAAGCCATC). Primary cells were transplanted into 7- to 8-week-old female NOD/SCID mice via tail vein. The tumor burden mice showed splenomegaly, and percentage of CD19$^+$ cells was higher than 80% in peripheral blood. Spleen blasts were retransplanted into a new batch of NOD/SCID recipients with 1×10^6 cells.

Four-week toxicity on SD rats and beagle dogs and hERG blockade assay

The West China-Frontier PharmaTech Co., Ltd. performed 4-week toxicity study according to GLP regulations. The effect of the purinostat mesylate on hERG was performed by Shanghai Chempartner Co., Ltd. Details are provided in Supplementary Methods.

HDAC enzymes and kinase inhibition assays, cell proliferation, apoptosis, cell cycle, Western blot, IHC, hematoxylin and eosin (H&E) staining, terminal deoxynucleotidyl transferase–mediated dUTP nick end labeling (TUNEL) staining, and flow cytometry for tumor burden, tissue distribution, and pharmacokinetic/pharmacodynamic study were described in detail in Supplementary Methods.

Statistical analysis

Statistical significance was assessed via GraphPad Prism Software 7.0., groups were compared using the *t* test, with $P < 0.05$ considered significant, and survival data were analyzed by a log-rank test (Mantel–Cox).

Results

Potent activity of purinostat mesylate *in vitro*

Purinostat mesylate has highly selective inhibition activity against class I and IIb HDAC subtypes. The IC_{50} values of purinostat mesylate were 0.81, 1.4, 1.7, and 3.8 nmol/L for class I HDAC1, 2, 3, and 8, and 11.5, 1.1 nmol/L for class IIb HDAC6 and 10, respectively (Fig. 1A). However, the IC_{50} of HDAC IIa and IV were 426–3,349 nmol/L (Fig. 1A). Compared with the five approved HDAC inhibitors, purinostat mesylate showed the highest inhibitory activity to class I and IIb (refs. 43, 44; Supplementary Table S1A). Although chidamide is a selective class I and HDAC10 subtype inhibitor, purinostat mesylate showed approximately 100-fold higher than chidamide inhibition on HDAC1, 2, 8, and 10 subtypes (ref. 45; Supplementary Table S1A). Meanwhile, purinostat mesylate at 1 μmol/L had no significant inhibitory activity on 89 kinase enzymes involved in tumor regulation (Supplementary Table S1B), suggesting highly selectivity of purinostat mesylate for HDAC class I and IIb subtypes.

To determine the IC_{50} values of purinostat mesylate against various hematologic tumor cell lines, we used LBH589 as positive control. We found that purinostat mesylate achieved better inhibitory effects than LBH589 on the most evaluated cell lines, with IC_{50} values at nanomolar or subnanomolar (Supplementary Table S2).

To further study the effects *in vitro* of Ph$^+$ leukemia cell lines, we exposed LAMA84 and BL-2 cells to different concentrations of purinostat mesylate. Purinostat mesylate significantly inhibited cell proliferation (Fig. 1B), induced apoptosis (Fig. 1C), and blocked cell-cycle progression at G_0–G_1 phase (Fig. 1D) in a dose-dependent manner. Consistent with previous reports (26, 43), purinostat mesylate effectively increased the levels of Ac-H3, Ac-H4, and decreased HSP90 in a concentration-dependent manner (Fig. 1E). BCR-ABL and c-MYC levels were downregulated as the purinostat mesylate concentration increased. Consistent with the BCR-ABL downregulation, p-SRC and STAT5 were also significantly suppressed. Importantly, we found that the SRC kinase HCK was significantly downregulated after purinostat mesylate treatment (LYN and BLK were not affected). These results indicated that purinostat mesylate had a potent therapeutic effect on Ph$^+$ leukemia by targeting BCR-ABL–dependent and -independent manners.

Purinostat mesylate exerted the robust antitumor activity on Ph$^+$ B-ALL

To investigate *in vivo* effect of purinostat mesylate against Ph$^+$ B-ALL, we developed a secondary transplantation model using GFP-labeled *BCR-ABL*–induced B-ALL cell line, named BL-2. BL-2 cells were injected into nonirradiated C57BL/6 recipient mice. Mice were randomly divided into four groups ($n = 10$ per group) when the leukemia cells (GFP$^+$B220$^+$) reached 12.6% ± 2.98% in peripheral blood on day 12, and then treatment with vehicle, LBH589 10 mg/kg, purinostat mesylate 5 and 10 mg/kg, three times a week for 5 weeks, respectively (Fig. 2A). Both purinostat mesylate and LBH589 statistically and significantly prolonged the overall survival (OS) and suppressed leukemia progression of mice compared with vehicle (Fig. 2A and B). The median OS were, respectively, 25.5 days in purinostat mesylate–treated (5 mg/kg) and 29.5 days in LBH589-treated (10 mg/kg) groups versus 18.5 days in the vehicle group. The OS of purinostat mesylate at 10 mg/kg treated group was significantly longer and 60% (6/10) of mice still survived at 100 days (Fig. 2A, right). After 5 weeks of LBH589 or purinostat mesylate treatment, GFP$^+$B220$^+$ cells almost disappeared in peripheral blood of the surviving mice (Fig. 2B, day 47). Importantly, one week after purinostat mesylate or LBH589 stopped treatment, no tumor cell in peripheral blood was detected (Fig. 2B, day 54), and even on day 100, the mice survived well (Fig. 2A, right).

To deeply analyze how the mice had progressive leukemia during the purinostat mesylate treatment and further reveal its antitumor mechanism, a more malignant BL-2 secondary transplantation mouse model was established again. Mice were divided into seven groups ($n = 4$) when GFP$^+$B220$^+$ cells reached 17.2% ± 7.19% in peripheral blood on day 14 (Supplementary Fig. S1A), treated with vehicle or purinostat mesylate (10 mg/kg) intravenously three times a week, and sacrificed 8 hours after treatment with at days. We found that GFP$^+$B220$^+$ cells in the spleens were completely eliminated only on day 3 with two times purinostat mesylate treatment and this complete inhibition was maintained for 26-day duration of the treatment. Consistent with the decreased GFP$^+$B220$^+$ percentages, the weights of the spleens were significantly decreased (Fig. 2C and D). At day 19, the weights of the spleens were almost identical to that of the healthy mice (Fig. 2D). Furthermore, purinostat mesylate therapy resulted in significant reduction in the proportion of GFP$^+$B220$^+$ cells in the BM (Fig. 2E). Then, we further isolated BM cells from the mice with progressive disease to analyze the changes of key protein levels. The red and blue dots in each group represent the poor response to purinostat mesylate treatment (Fig. 2E). Consistent with *in vitro* results, purinostat mesylate increased Ac-H3 and Ac-H4, and decreased the BCR-ABL, HSP90, HCK, p-SRC, and c-MYC levels in BM cells (Fig. 2F and G). However, for the D8-3 (the third mouse after treatment 4 times), D12-4 (the fourth mouse after

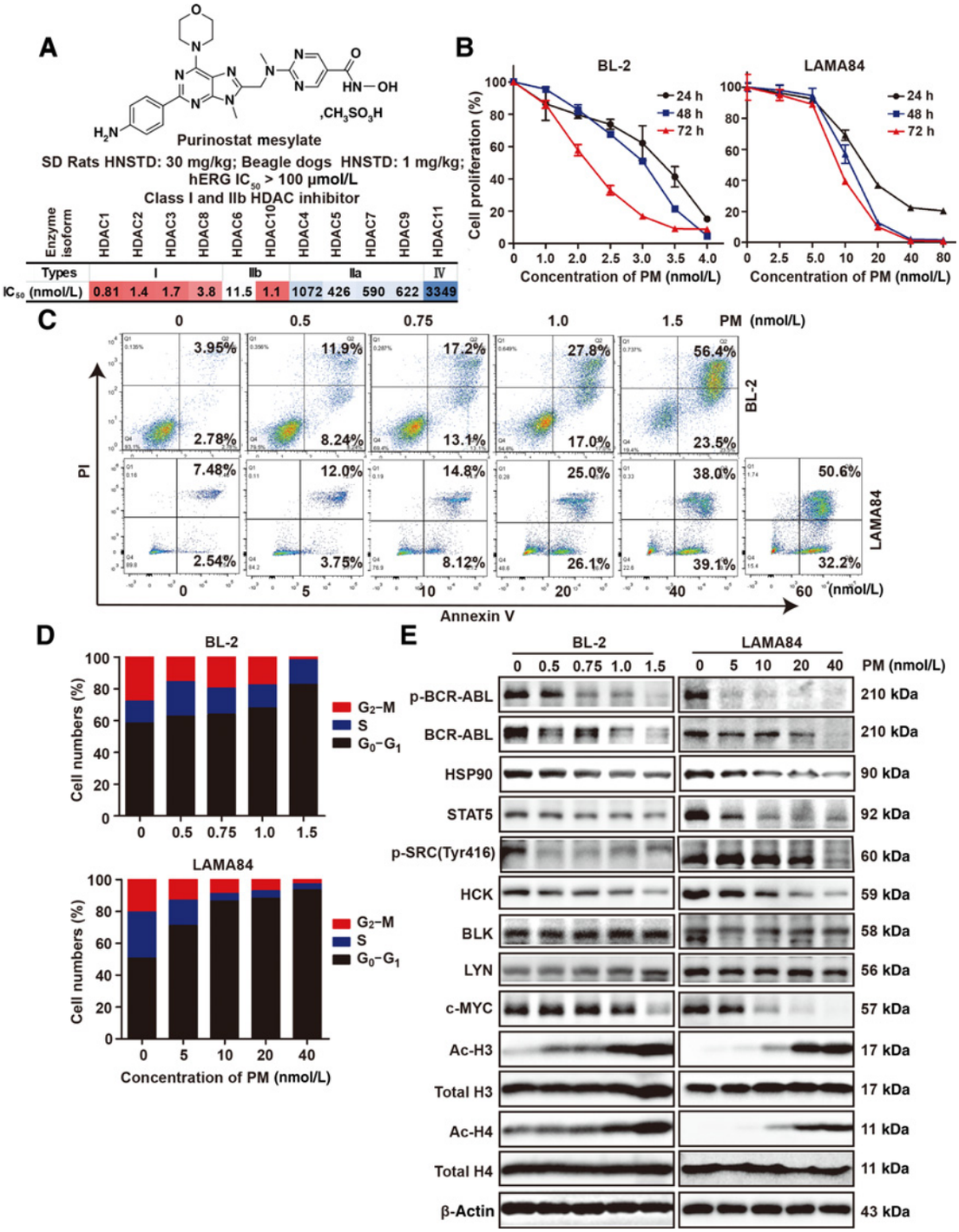

Figure 1.

Class I/IIb HDAC inhibitor purinostat mesylate showed potent activity *in vitro*. **A,** Chemical structure and selectivity profile of purinostat mesylate against HDAC subtypes. **B,** Proliferation of BL-2 and LAMA84 in the presence of increasing concentrations of purinostat mesylate (0–4 nmol/L for BL-2; 0–80 nmol/L for LAMA84) for 24, 48, and 72 hours, respectively. Error bars indicate SD from three replicates. **C,** Induction of apoptosis with different concentrations of purinostat mesylate in BL-2 and LAMA84 cell lines for 24 hours. **D,** Cell cycle in BL-2 and LAMA84 cell lines treated with different concentrations of purinostat mesylate for 24 hours. **E,** BL-2 and LAMA84 cells were exposed to increasing concentrations of purinostat mesylate for 24 hours, and the BCR-ABL, p-BCR-ABL, HSP90, STAT5, HCK, BLK, LYN, p-SRC(Tyr416), c-MYC, Ac-H3, and Ac-H4 protein levels were detected by Western blot analysis. β-Actin was used as loading control.

2-week treatment), and D19-4 (the fourth mouse after 3-week treatment) mice, BCR-ABL levels were relatively low, while p-SRC and c-MYC levels were high. In addition, D5-2 mouse had minimal upregulation of Ac-H3 and Ac-H4, and accompanied high BCR-ABL level. Thus, these protein markers have significant implications whether Ph$^+$ B-ALL mice respond well to purinostat mesylate. In addition, as shown in Fig. 2H, after three weeks of purinostat mesylate treatment (day 19), the mice showed normal organ morphology (normal splenic follicular architecture and no leukemic cell infiltration into BM). Overall, these results indicated that purinostat mesylate exerted a robust activity in the Ph$^+$ BL-2 mouse model *in vivo* via inhibiting the tumor cell proliferation and suppressing HSP90, BCR-ABL, and its downstream partners.

Purinostat mesylate is mainly concentrated in tumor tissues

Pharmacokinetics and pharmacodynamics of purinostat mesylate were performed in BL-2 secondary transplantation model. On day 14 postinjection, 7 mice per group with 17.1% ± 1.69% GFP$^+$B220$^+$ cells in peripheral blood (Supplementary Fig. S1C) were given a single dose of purinostat mesylate (10 mg/kg i.v.). As shown in Fig. 3A, the concentrations of purinostat mesylate in all examined tissues showed a decrease with time. Purinostat mesylate was mainly distributed in the intestine, lung, kidney, stomach, and spleen. Interestingly, the concentration of purinostat mesylate in spleen remained high for 24 hours (Fig. 3A; Supplementary Table S3). Similar results were also observed in bone marrow cells: the concentration of purinostat mesylate in BM cells was kept high at 24 hours with purinostat mesylate of 82.2 ± 16.4 ng/10^8 cells (Fig. 3A, right). As shown in Table 1, the AUC_{0-72h} of plasma, spleen, and BM cells were 501 ± 72.0 ng/mL/hour, 8,949 ± 1,354 ng/g/hour, and 3,968 ± 589 ng/10^8 cell/hour, respectively. The $t_{1/2}$ of plasma, spleen, and BM cells were 1.34 ± 1.22, 18.6 ± 2.79, and 28.3 ± 8.34 hours, respectively, indicating that purinostat mesylate eliminated rapidly in plasma, and accumulated in tumor tissues such as spleen and BM, which contained more leukemia cells. Similarly, purinostat mesylate in spleen and BM cells showed longer MRT_{0-72h} and smaller CL_Z compared with plasma, suggesting the potential of purinostat mesylate for antitumor efficacy with decreased systemic toxicity. In addition, in the BM cells, the acetylation levels of H3 and H4 increased and reached the highest at 8 hours, which was 7.25-fold and 14.6-fold of the vehicle group, and the histone acetylation increased for at least 72 hours (Fig. 3B and C; Supplementary Fig. S1D). These findings are indicative of a sustained target effect during dose intermission, providing the evidence for less-frequent dosing treatment of purinostat mesylate.

Twenty-four hours after purinostat mesylate treatment, GFP$^+$B220$^+$ cells in spleen and BM decreased from 17.3% ± 1.18% and 69.0% ± 3.09% to 7.83% ± 0.940% and 56.5% ± 2.22%, respectively (Fig. 3F and I). At 48-hour treatment, the tumor cells in spleens and BM continually decreased to 3.00% ± 1.19% and 48.60% ± 1.19%, respectively. After 72 hours of administration, leukemia cells began to increase represented as 10.8% ± 2.60% and 56.1% ± 0.991% in spleens and BM, respectively. These results suggested that it was necessary to administrate purinostat mesylate three times a week. Furthermore, 24 hours post purinostat mesylate administration, similar to the $t_{1/2}$ time point of spleen and BM, showed promising efficacy as evidenced by the significant reduction of spleen weights and relatively normal follicular architecture (white medulla) compared with that of vehicle (Fig. 3D and E). TUNEL staining of spleens showed that purinostat mesylate considerably induced tumor cells' apoptosis (Fig. 3G). IHC analyses from spleens showed that the protein levels of KI67 and c-MYC were significantly downregulated, and the levels of Ac-H3 and Ac-H4 were upregulated (Fig. 3H). Western blot analysis of BM cells revealed that Ac-H3 and Ac-H4 levels were elevated and BCR-ABL, HSP90, p-SRC, HCK, and c-MYC levels were decreased 24 hours post-treatment (Fig. 3J). Overall, these results indicated that purinostat mesylate possessed favorable pharmacokinetic properties in BL-2–bearing mice, which was contributed to improve its antitumor ability and reduce toxicity.

Purinostat mesylate showed potent antileukemia effects in *BCR-ABL(T315I)*–induced primary B-ALL mice

Clinically, *BCR-ABL(T315I)* mutation is the most common resistance to TKIs. To assess the antitumor efficacy of purinostat mesylate, we employed a *BCR-ABL(T315I)*–induced primary B-ALL mouse model (Fig. 4A). At day 12 post BM transplantation (BMT), 18.9% ± 6.03% of GFP$^+$B220$^+$ cells were detected in peripheral blood (Fig. 4C). Then, model mice were randomly divided into three groups and treated with purinostat mesylate or vehicle for 8 weeks. Purinostat mesylate both at 5 and 10 mg/kg significantly prolonged the survival of *BCR-ABL(T315I)*–induced B-ALL mice (Fig. 4B). The median OS of the vehicle group was 42 days, while all mice in the purinostat mesylate treatment groups survived leukemia cell free. Two weeks posttreatment, leukemia cells in the purinostat mesylate treatment groups were almost not detected in the peripheral blood, while a large number of leukemia cells existed in the vehicle mice (Fig. 4C, day 24). The mice in the vehicle group showed moribund states with severe paralysis of hind limbs and splenomegaly. In contrast, the mice treated with purinostat mesylate survived well and the size of spleens became normal (Supplementary Fig. S2A). H&E staining of spleens showed that there was a large number of leukemia cell infiltration in the vehicle group, while the spleens showed normal follicular architecture in the purinostat mesylate–treated groups (Supplementary Fig. S2B). Furthermore, we analyzed the leukemia progression in spleen and BM within 2 weeks purinostat mesylate treatment. As shown in Fig. 4D, E, and G, after 2 doses (day 3), leukemia cells were significantly decreased in peripheral blood (62.6% ± 10.4% vs. 4.68% ± 4.76%), spleen (60.5% ± 13.7% vs. 10.47% ± 5.25%) and BM (77.7% ± 7.86% vs. 8.01% ± 5.46%), consistent with the results of H&E staining of BM and spleen shown in Fig. 4I. After treatment for 2 weeks, the leukemia cells almost disappeared in peripheral blood, spleen, and BM, and the weight (0.08 ± 0.03 g) of spleens became normal (Fig. 4D–G). Mechanistically, purinostat mesylate obviously increased the acetylation levels of H3 and H4 in BM at 8 and 24 hours post purinostat mesylate treatment (Fig. 4H). BCR-ABL(T315I), HSP90, c-MYC, p-SRC, and HCK were significantly downregulated (Fig. 4H). After 8 weeks of continuous treatment, no GFP$^+$B220$^+$ cells were detected in peripheral blood (Fig. 4C, day 65). It is worthy to mention that when treatment was stopped, the mice still remained healthy at the end of the study on day 122 (Supplementary Fig. S2C), indicating that purinostat mesylate completely inhibited tumor recurrence. Furthermore, spleen and pleural effusion cells were isolated from diseased mice and treated with purinostat mesylate for 24 hours *in vitro* (Supplementary Fig. S2D). The results showed that purinostat mesylate at 2.5 and 5 nmol/L decreased spleen tumor cells from 36.5% to 6.75% and 1.91%, respectively. Pleural effusion tumor cells were decreased

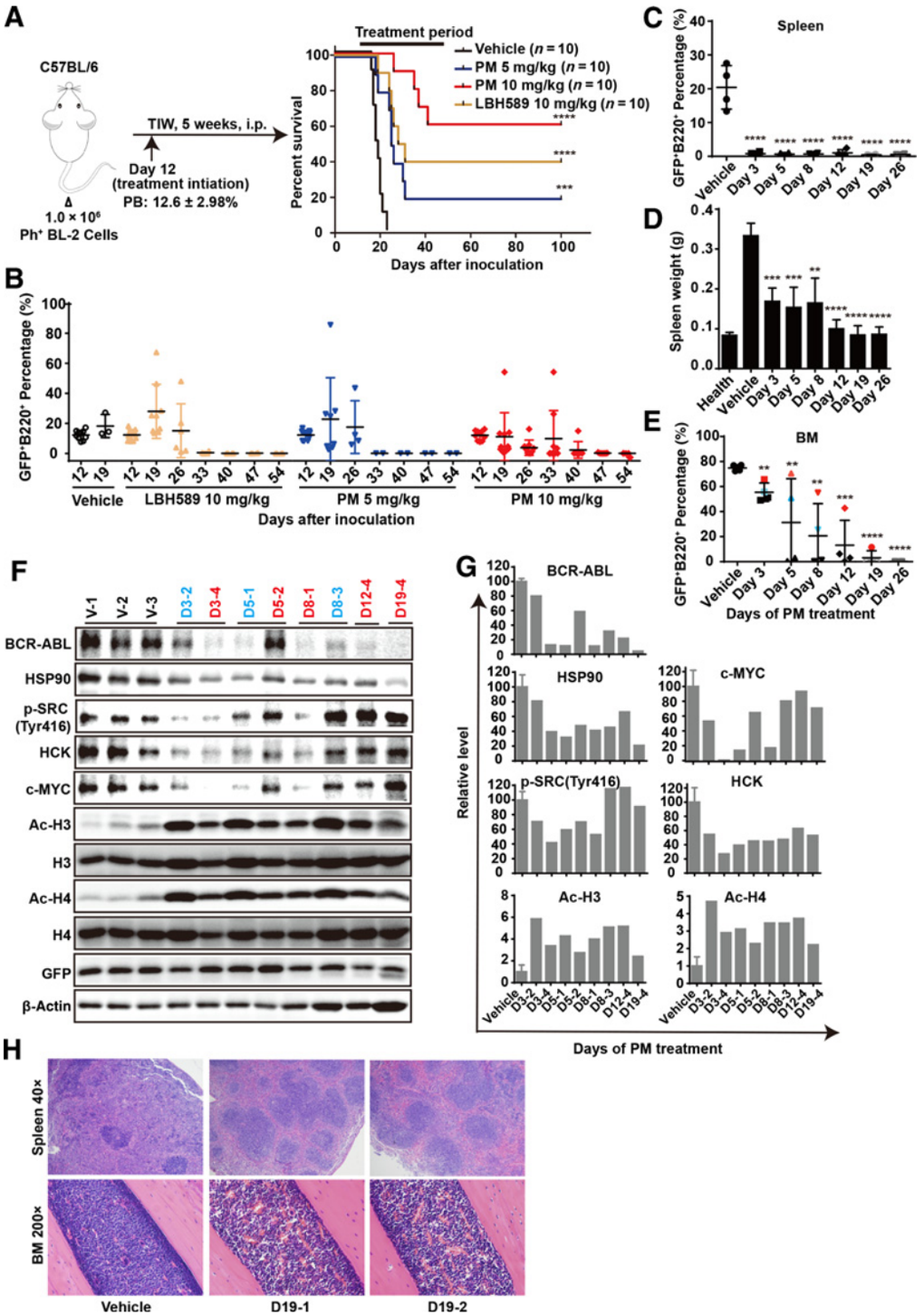

Figure 2.

Antileukemic effects of purinostat mesylate (PM) in a BL-2 secondary transplantation mouse model of Ph$^+$ B-ALL. **A,** Kaplan–Meier survival curves of Ph$^+$ BL-2–bearing mice treated with vehicle, LBH589 10 mg/kg, purinostat mesylate 5 and 10 mg/kg, 10 mice per group. Twelve days after inoculation (12.6% ± 2.98% of GFP$^+$B220$^+$ cells in peripheral blood), the mice started treatment via intraperitoneal route, three times a week, and continued for 5 weeks. Treatment begins on day 12 and ends on day 47. The difference in survival between treatment and vehicle groups is highly significant (****, $P < 0.0001$; ***, $P < 0.001$; Mantel–Cox test). **B,** FACS analysis of the percentage of GFP$^+$B220$^+$ cells in peripheral blood after weekly administration of all surviving Ph$^+$ BL-2–bearing mice. **C–E,** Fourteen days after inoculation, Ph$^+$ BL-2–bearing mice were FACS analyzed and divided into seven groups ($n = 4$) with the same tumor burden 17.2% ± 7.19% of GFP$^+$B220$^+$ in peripheral blood. (*Continued on the following page.*)

from 92.7% to 1.13% by purinostat mesylate at 0.25 nmol/L. In addition, we also assessed the antitumor efficacy of purinostat mesylate in *BCR-ABL(WT)* B-ALL mouse model. As shown in Supplementary Fig. S2E, the vehicle group died within 9 weeks (median OS, 52.5 days) after BMT; however, no mice died in purinostat mesylate treatment group. The number of total white cells decreased, and the percentage of GFP$^+$B220$^+$ cells in peripheral blood almost disappeared post purinostat mesylate treatment for 3 weeks (Supplementary Fig. S2F and S2G). These results showed that purinostat mesylate also had excellent antitumor efficacy in this model. Taken together, these results demonstrate that purinostat mesylate exhibits superior therapeutic efficiency on Ph$^+$ B-ALL, including T315I-mutated B-ALL.

Purinostat mesylate exerted potent activity on primary Ph$^+$ B-ALL cells from patients

To determine purinostat mesylate activity on primary cells of Ph$^+$ B-ALL, we obtained peripheral blood from Ph$^+$ B-ALL patient #1 with T315I mutation who relapsed after CAR-T treatment, and Ph$^+$ B-ALL patient #2 harboring *IKZF1* exon deletion who relapsed after TKI combined with IFNγ treatment (Supplementary Fig. S2H and S2I). Purinostat mesylate effectively induced 65.1% and 84.0% apoptosis of the primary cells in patient #1 after exposure to 20 nmol/L purinostat mesylate for 24 and 48 hours, respectively, and the levels of BCR-ABL(T315I) and c-MYC were also decreased (Fig. 5A and B). Similar results were also observed in the cells of patient #2: purinostat mesylate induced apoptosis of 26.59% and 44.04% at 5 and 10 nmol/L for 24 hours, respectively (Fig. 5A). Although HSP90 levels did not change, Ac-H3 and Ac-H4 were increased, and BCR-ABL, c-MYC, p-SRC, and HCK levels were significantly decreased in a dose-dependent manner (Fig. 5B). These results indicated that purinostat mesylate effectively induced apoptosis both in Ph$^+$ WT and T315I-mutated B-ALL cells from patient samples via suppressing multiple signaling pathways.

To further investigate purinostat mesylate antileukemia activity, primary cells of patient #2 were used to generate a PDX model. On day 33 postxenograft, the percentages of CD19$^+$ cells in peripheral blood reached to 24.2% ± 8.26% (Supplementary Fig. S1E). Diseased mice were randomly divided into three groups and treated with vehicle or purinostat mesylate. As shown in Fig. 5C, purinostat mesylate 2.5 and 10 mg/kg significantly prolonged the survival of Ph$^+$ B-ALL–bearing mice. The median OS of the vehicle mice was 21 days, while for purinostat mesylate 2.5 and 10 mg/kg treatment groups, it was 66 and 73 days, respectively. As expected, purinostat mesylate significantly reduced total white blood cells and CD19$^+$ cells in peripheral blood (Fig. 5D and E). Furthermore, after 3-week treatment, the splenomegaly was markedly reduced in mice receiving purinostat mesylate 2.5 and 10 mg/kg, with masses of 0.495 ± 0.075 g and 0.271 ± 0.066 g, respectively, while the vehicle spleen was 0.956 ± 0.160 g (Fig. 5F). Consistent with *in vitro* results, Ac-H3 and Ac-H4 were increased, and the levels of BCR-ABL, c-MYC, p-SRC, and HCK were also significantly downregulated in the spleens of purinostat mesylate–treated groups (Fig. 5G). These results showed that purinostat mesylate was effective in Ph$^+$ B-ALL PDX model mice, and indicated that purinostat mesylate had the potential to be used in the clinical treatment of Ph$^+$ B-ALL patients who relapse post TKI treatment.

Purinostat mesylate exhibited favorable toxicology profiles

To evaluate purinostat mesylate preclinical long-term toxicity, purinostat mesylate was administrated intravenously at doses of 0, 3, 10, and 30 mg/kg for SD rats, and 0, 0.3, 1, and 3 mg/kg for beagle dogs. The results showed that the highest nonseverely toxic dose (HNSTD) of purinostat mesylate was 30 mg/kg in SD rats and 1 mg/kg in beagle dogs. Except for the 4 beagle dogs that died in 3 mg/kg group ($n = 10$), all animals survived in good condition in the other groups. The body weights of 30 mg/kg rats and 1 mg/kg beagle dogs decreased slightly during the dosing phase, while no significant differences were noted at the end of recovery phase (Supplementary Fig. S3A and S3B). Evaluation of 22 hematologic parameters indicated that only male rats had a decrease on the levels of mean corpuscular hemoglobin (MCH) and mean corpuscular hemoglobin concentration (MCHC), and RBC increased to the edge of the normal range (Supplementary Table S4-1). Consistently, among the 24 clinical chemistry parameters, there was no significant abnormality in the results of the female rats, and only increased urea and phosphorus (P) in male rats in the normal range (Supplementary Table S4-2). As shown in Supplementary Table S4-3, the percentage of lymphocytes decreased and eosinophil increased at the end of the dosing period, and no significant abnormality was observed at the end of the recovery period. Consistent with the SD rats, the body weights (Supplementary Fig. S3B), hematologic parameters (Supplementary Table S4-4), clinical chemistry parameters (Supplementary Table S4-5), BM cell percentages, and megakaryocyte counts (Supplementary Table S4-6) in beagle dogs of 0.3 and 1 mg/kg groups, compared with the control group, few differences were observed at the end of dosing phase and no significant abnormality at the end of the recovery period.

To understand the toxicities of purinostat mesylate displayed in moribund beagle dogs in 3 mg/kg group, we conducted a further analysis. These dogs mainly displayed the following symptoms with different degrees: decreased activity, food emesis, increased salivation, dark red unformed feces, and decreased food consumption. Clinical pathology parameters UREA, CREA, P, LDL, LIPC, GLU were increased, APTT was prolonged, and WBC, NEU, LYM, MONO, EOS, PLT, RET, Ca^{2+}, Na^+, and Cl^- were decreased (Supplementary Table S4-4 and S4-5). The morphologic pathology results showed that the moribund dogs were mainly showed a decrease in

(*Continued.*) Mice were treated with purinostat mesylate (10 mg/kg) intravenously three times a week, and respectively sacrificed at 8 hours of purinostat mesylate administration at day 0 (vehicle), day 3 (two times treatment), day 5 (one week treatment), day 8 (four times treatment), day 12 (two weeks treatment), day 19 (3 weeks treatment), and day 26 (1 month treatment). The tumor cell burden (GFP$^+$B220$^+$) in spleen (**C**), BM (**E**), and spleen weights (**D**) were analyzed. Each point represents the mean value of 4 individual mice ± SD (**, $P < 0.01$; ***, $P < 0.001$; ****, $P < 0.0001$; $n = 4$, t test), compared with vehicle. **F,** BM cells were collected from diseased mice in the purinostat mesylate (10 mg/kg) treatment and vehicle groups, respectively. The tumor burden of red-numbered corresponds to the red dot in **E**, and the tumor burden of blue-numbered corresponds to the blue dot in **E**. For example, D19-4 represents the fourth mouse on day 19 group (3-week treatment). Western blot analysis the protein levels of BCR-ABL, HSP90, p-SRC(Tyr416), c-MYC, HCK, Ac-H4, and Ac-H3. The percentages of GFP$^+$B220$^+$ in BM were used to adjust the number of tumor cells to be consistent. **G,** Relative quantification of protein levels in **F**, GFP as quantitative control. **H,** Photomicrographs of H&E stain of spleen and BM sections from vehicle and purinostat mesylate–treated mice after 3 weeks treatment (day 19).

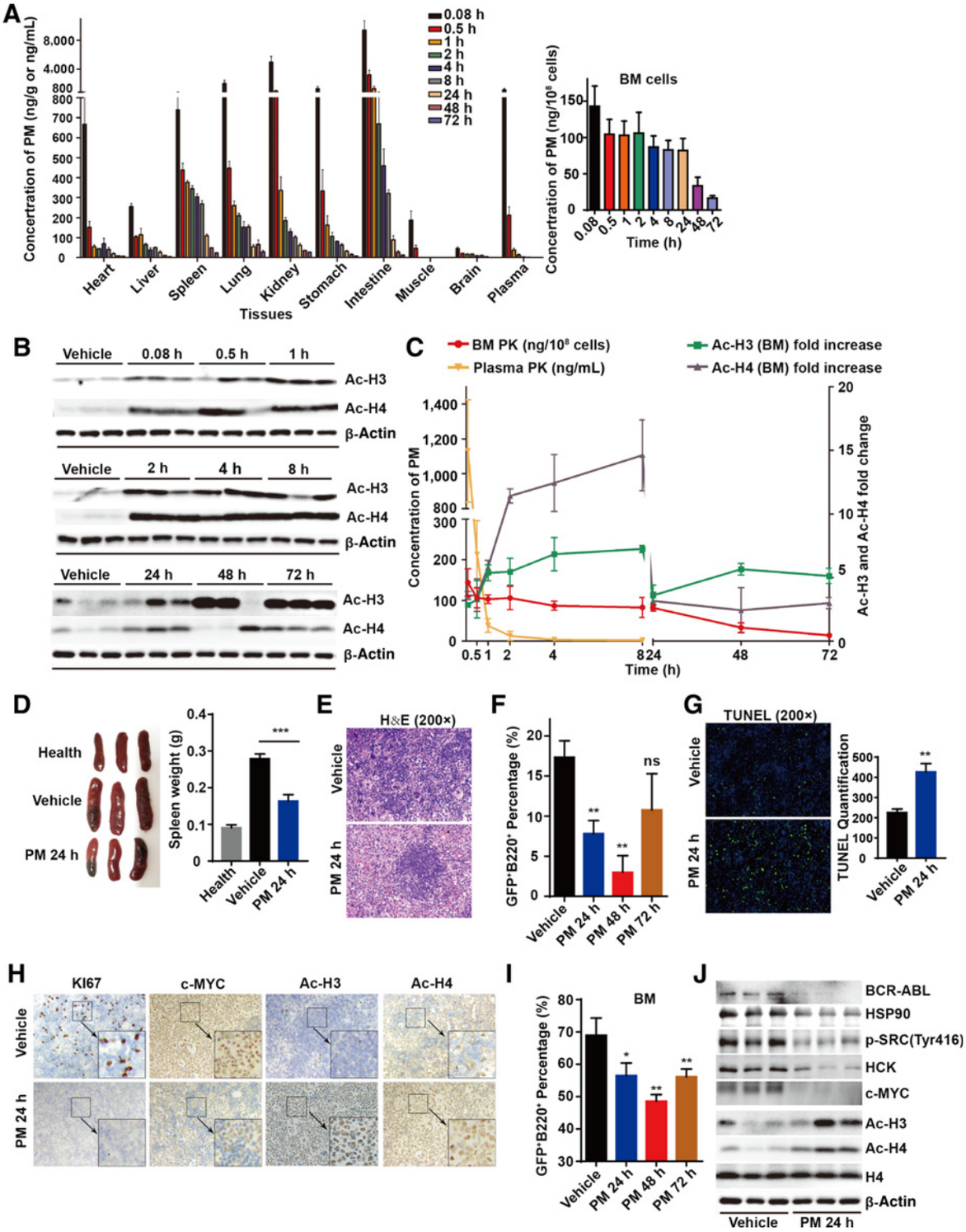

Figure 3.

Pharmacokinetics and pharmacodynamics of purinostat mesylate (PM) in the BL-2 secondary transplantation model of Ph^+ B-ALL. Fourteen days after inoculation, Ph^+ BL-2–bearing mice were FACS analyzed and divided into 10 groups ($n = 7$) with the same tumor burden (17.1% ± 1.69% of GFP^+B220^+ in PB); mice were sacrificed at different time points (0–72 hours) after a single purinostat mesylate 10 mg/kg i.v. administration. **A,** Purinostat mesylate concentration in organizations in the BL-2–bearing mice ($n = 4$). **B,** Acetylation H3 and acetylation H4 analysis in BM cells from the BL-2–bearing mice at different time ($n = 3$). **C,** Pharmacokinetic/pharmacodynamic statistics of purinostat mesylate in BM cells and plasma. (*Continued on the following page.*)

Table 1. Pharmacokinetic parameters of purinostat mesylate after a single intravenous administration to BL-2 bearing mice (mean ± SD; $n = 4$)

Parameters	Plasma	Spleen	Bone marrow
$AUC_{0\text{-}t}$ (ng/mL/h or ng/g/h or ng/10^8 cell/h)	501 ± 72.0	8,949 ± 1,354	3,968 ± 589
$AUC_{0\text{-}\infty}$ (ng/L/h or ng/g/h or ng/10^8 cell/h)	503 ± 69.8	9,512 ± 1,433	4,601 ± 657
$MRT_{0\text{-}t}$ (h)	0.425 ± 0.080	17.5 ± 1.93	25.1 ± 1.42
$MRT_{0\text{-}\infty}$ (h)	0.513 ± 0.166	23.0 ± 2.61	37.5 ± 8.34
$t_{1/2z}$ (h)	1.34 ± 1.22	18.6 ± 2.79	28.3 ± 8.34
CL_z (L/h/kg)	20.2 ± 2.58	1.07 ± 0.143	2.21 ± 0.355
C_{max} (ng/mL or ng/g or ng/10^8 cell)	1,131 ± 294	741 ± 155	142 ± 30.0

hematopoietic cells in BM and a decrease in lymphocytes in the spleen, intestinal lymphoid tissue, mesenteric lymph node, and cervical lymph node (Supplementary Fig. S3C). Therefore, the death of beagle dogs was probably attributed to the toxicity of high doses of purinostat mesylate on immune and hemopoietic systems.

In addition, in *in vitro* hERG testing, no obvious inhibition was observed at the highest tested concentration of 100 μmol/L (Supplementary Fig. S3D). In summary, these results indicate that purinostat mesylate shows highly favorable toxicology profiles for preclinical study.

Discussion

In this study, we reported a novel class I and IIb HDAC-selective inhibitor purinostat mesylate, which had superior efficiency against Ph$^+$ leukemia, especially on Ph$^+$ B-ALL (including WT and T315I mutation) both *in vitro* and *in vivo*. Purinostat mesylate exhibited superior efficiency against Ph$^+$ leukemia in LAMA84 and BL-2 cell lines, as well as in primary Ph$^+$ (including WT and T315I mutation) B-ALL cells obtained from relapsed patients. The levels of BCR-ABL and acetylation of H3 and H4 were significantly altered during purinostat mesylate treatment, which may potentially be used as biomarkers to assess its therapeutic efficacy for Ph$^+$ B-ALL. Critical oncoproteins for Ph$^+$ B-ALL pathogenesis, such as BCR-ABL, HCK, c-MYC, STAT5 (29, 46–48), were significantly downregulated by purinostat mesylate both *in vitro* and in *vivo*. Purinostat mesylate also decreased HSP90 protein level. Previous studies already demonstrated that HSP90 was also a potential target for Ph$^+$ leukemia therapy (2, 49). These results well explained the reason that purinostat mesylate achieved promising therapeutic outcome for Ph$^+$ B-ALL.

Taking the advantages of different disease mouse models, we employed three kinds of Ph$^+$ B-ALL models to evaluate purinostat mesylate pharmacodynamic properties. The advantages of GFP$^+$ BL-2 secondary engraft mouse model are easy to induce, with highly malignant and the recipients holding normal immune system. These properties contribute significantly to assess purinostat mesylate pharmacodynamic characteristics during treating Ph$^+$ B-ALL. It is worth noting that some recipients still had progressive leukemia during the purinostat mesylate treatment period (Fig. 2B and E). The reasons may be that the BL-2 cell came from pleural effusion of primary Ph$^+$ B-ALL mice with highly malignant, and during *in vitro* culturing, unknown mutations and cell variability were further accumulated. The hypothesis was further confirmed by analyzing leukemia cells isolated from recipients that did not respond well to purinostat mesylate. We found these leukemia cells owned low level of BCR-ABL, high level of c-MYC and SRC family kinases, as well as low acylation level of H3 and H4 (Fig. 2F and G). These results indicated that mutated genes might cause cells to poorly absorb purinostat mesylate. Others resistance mechanisms are still unclear, such as leukemia cells from D5-1 and D8-1 mice possessed higher Ac-H3 and Ac-H4 levels and lower BCR-ABL, HSP90, c-MYC, and p-SRC levels, but disease also progressed during treatment. These disadvantages of BL-2 model were well compensated by *BCR-ABL*–induced primary B-ALL model. All recipients completely responded to purinostat mesylate during treatment (Supplementary Fig. S2E). In Ph$^+$ T315I mutation B-ALL mouse model, in only 2 weeks of treatment with 5 mg/kg purinostat mesylate, leukemia cells in the peripheral blood almost disappeared and leukemia did not relapse when the administration was stopped for 8 weeks. These results indicate that purinostat mesylate is also highly effective against T315I-mutated Ph$^+$ B-ALL. Purinostat mesylate also displayed promising therapeutic effects on Ph$^+$ B-ALL including leukemia cells with *BCR-ABL(T315I)* and *IKZF1* exon deletion. In PDX models derived from relapsed Ph$^+$ B-ALL patient post TKI treatment with *IKZF1* exon 4–7 deletion mutation (Supplementary Fig. S2I), purinostat mesylate also significantly prolonged the survival of the PDX model mice. These two mutations represent clinically most severe situations for patients with Ph$^+$ B-ALL. Moreover, we speculate that purinostat mesylate used as a first-line treatment for Ph$^+$ B-ALL before using other protocols may achieve more amazing effects. Thus, purinostat mesylate is a promising candidate drug for clinical studies in patients with Ph$^+$ B-ALL.

For pharmacokinetic/pharmacodynamic study, percentage of the leukemia cells from spleen and BM were found to reach the lowest point at 48 hours postadministration. Therefore, the dosage regimen should be once every other day (three times a week). Moreover, purinostat mesylate was fast cleared from the plasma, and it appeared to accumulate in spleen and BM, and the concentration of purinostat mesylate in spleen and BM cells maintains highly at 48 hours after dosing. Similarly, the $t_{1/2}$ in plasma was 1.34 hours, while 18.6 hours and 28.3 hours in spleen and BM. These pharmacokinetic/pharmacodynamic properties may support purinostat mesylate for once every other day dosing

(*Continued.*) **D,** Mice were sacrificed after 24 hours of purinostat mesylate treatment, and compared with the size (left) and weight (right) of the spleens with vehicle mice. ***, $P < 0.001$ ($n = 3$, t test). **E,** Spleens were taken out for H&E staining at 24 hours of purinostat mesylate treatment compared with vehicle mice. Pictures were taken with (200 ×) magnification. **F,** FACS analyzed the percentage of GFP$^+$B220$^+$ cells of spleens at 24, 48, and 72 hours after a single purinostat mesylate 10 mg/kg i.v. administration. **, $P < 0.01$ ($n = 3$, t test), compared with vehicle. **G,** Spleens were taken out for TUNEL staining at 24 hours of purinostat mesylate treatment compared with vehicle mice. Pictures were taken with (200 ×) magnification. Quantification of TUNEL stain per field (**G**, right). **, $P < 0.01$ ($n = 3$, t test). **H,** Spleens were taken out for IHC stain at 24 hours of purinostat mesylate treatment to analyze the marker (KI67, Ac-H3, Ac-H4, and c-MYC) level varieties. Pictures were taken with (200 ×) magnification. **I,** FACS analyzed the percentage of GFP$^+$B220$^+$ cells in BM at 24, 48, and 72 hours after a single intravenous purinostat mesylate (10 mg/kg) treatment. *, $P < 0.05$; **, $P < 0.01$ ($n = 3$, t test), compared with vehicle. **J,** BCR-ABL, HSP90, p-SRC(Tyr416), HCK, c-MYC, Ac-H3, and Ac-H4 levels analysis via Western blotting in BM cells from vehicle and a single purinostat mesylate 10 mg/kg treatment groups. β-Actin was used as loading control.

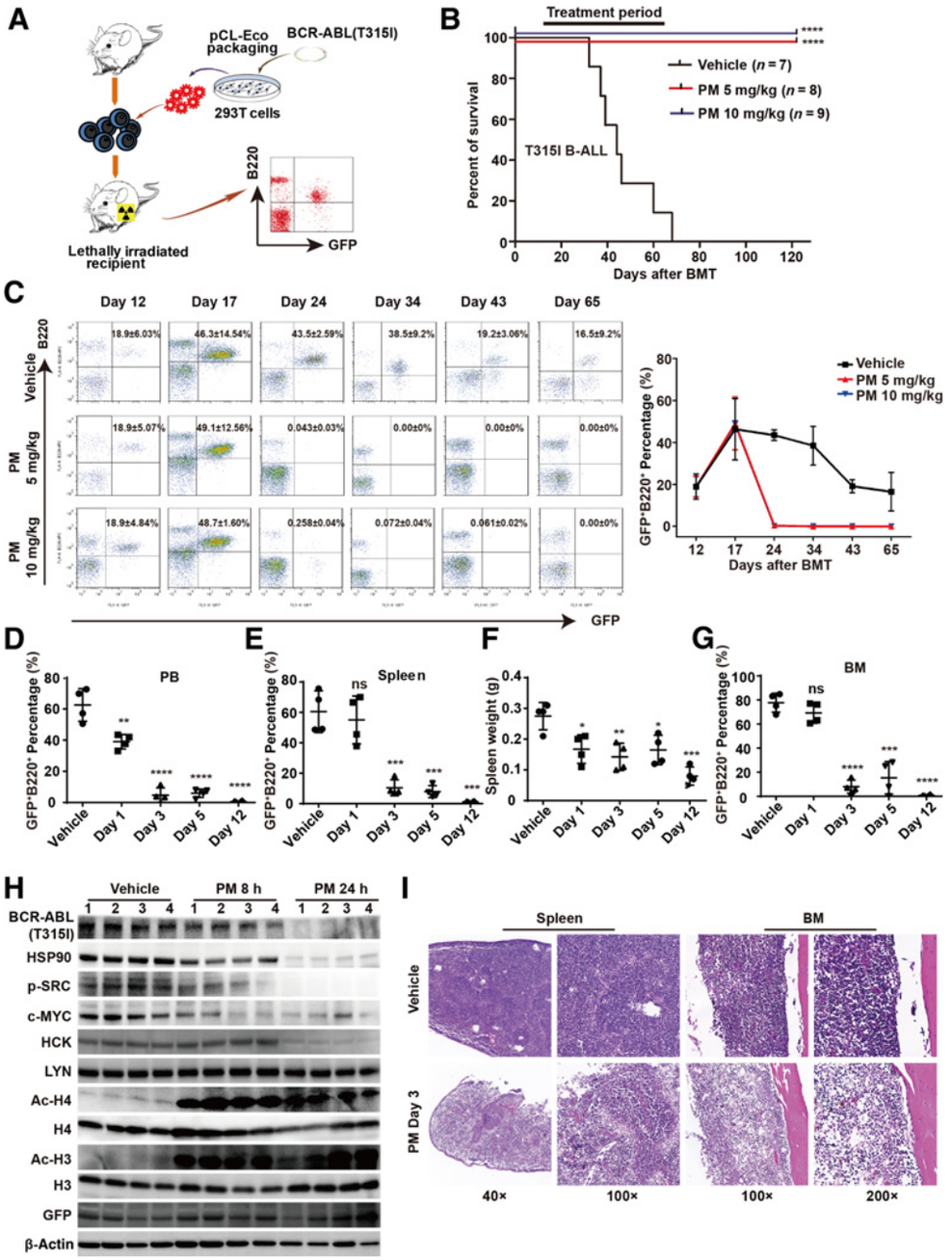

Figure 4.

Purinostat mesylate (PM) showed antileukemia effects in Ph$^+$ T315I mutation–induced primary B-ALL mouse model. **A,** The established method of the Ph$^+$ T315I mutation B-ALL mouse model. **B,** Kaplan–Meier survival curves of Ph$^+$ T315I mutation B-ALL–bearing mice treated with vehicle ($n = 7$), 5 mg/kg purinostat mesylate ($n = 8$), or 10 mg/kg purinostat mesylate ($n = 9$) are shown. Difference in survival between treatment and vehicle groups is highly significant. ****, $P < 0.0001$ (Mantel–Cox test). **C,** Twelve days after BMT, mice were randomized to begin treatment. FACS analysis shows percentage of GFP$^+$B220$^+$ cells in peripheral blood for the vehicle or purinostat mesylate–treated groups of Ph$^+$ T315I mutation B-ALL–bearing mice at different time points (left). Statistical analysis of the percentage of GFP$^+$B220$^+$ cells in peripheral blood of all mice with SD (right). Ph$^+$ T315I mutation B-ALL mouse model with more severe tumor burden was induced. After 16 days, all mice were FACS analyzed and divided into 5 groups with the same percentage (62.6% ± 10.4%) of GFP$^+$B220$^+$ in peripheral blood, 4 mice per group. Treatment with purinostat mesylate (10 mg/kg) intravenously three times a week. Mice were sacrificed at 8 hours of purinostat mesylate administration at day 1, day 3, day 5 (1-week treatment), and day 12 (2-week treatment). The tumor cell burden (GFP$^+$B220$^+$) in peripheral blood (**D**), spleen (**E**), BM (**G**), and spleen weight (**F**) were analyzed. Each point represents the mean value of 4 individual mice ± SD. *, $P < 0.05$; **, $P < 0.01$; ***, $P < 0.001$; ****, $P < 0.0001$ ($n = 4$, t test), compared with vehicle. **H,** Tumor burden mice treated with purinostat mesylate (10 mg/kg), at 8 and 24 hours; BM cells were collected. Western blotting analysis of BCR-ABL(T315I), HSP90, p-SRC(Tyr416), c-MYC, HCK, LYN, Ac-H4, and Ac-H3 protein level varieties, GFP, and β-actin as loading control. **I,** Photomicrographs of H&E stain of spleen and BM sections from vehicle and purinostat mesylate–treated mice (Day 3).

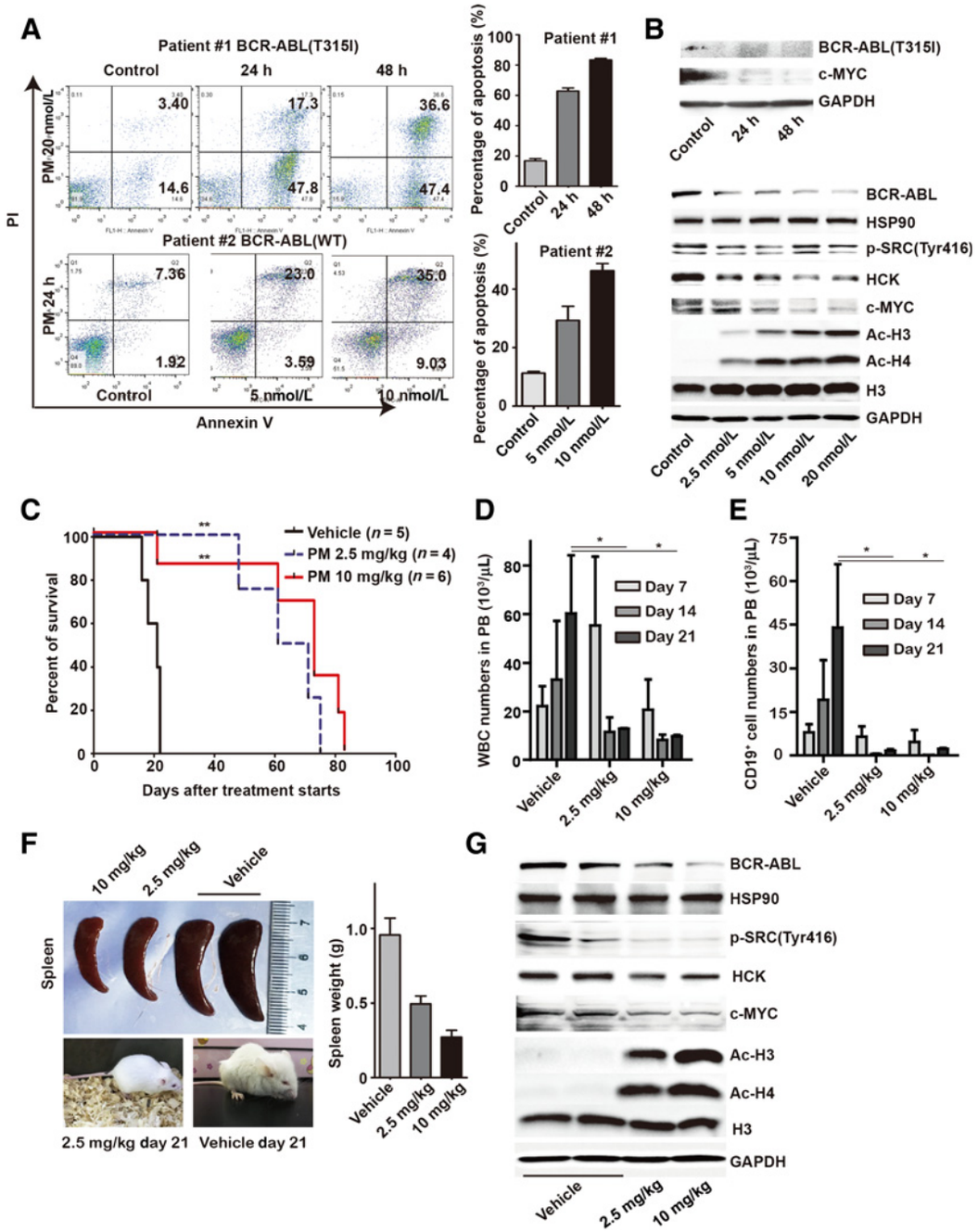

Figure 5.

Purinostat mesylate (PM) exerted potent activities on primary cells *in vitro* and in PDX model of Ph$^+$ B-ALL. **A,** Purinostat mesylate induces apoptosis of primary cells from Ph$^+$ T315I mutation B-ALL patient #1 and Ph$^+$ B-ALL patient #2 with *IKZF1* exons deletion (left); apoptosis statistics of patient #1 and #2 primary cells after purinostat mesylate treatment (right). **B,** Western blot analysis of the BCR-ABL(T315I) and c-MYC levels in patient #1 cells (top panel). Western blot analysis of the BCR-ABL, HSP90, p-SRC(Tyr416), c-MYC, HCK, Ac-H4, and Ac-H3 levels in patient #2 cells (bottom panel). The primary cells of patient #1 were treated with 20 nmol/L purinostat mesylate for 24 and 48 hours, and the primary cells of patient #2 were treated with purinostat mesylate (control, 2.5, 5, 10, and 20 nmol/L) for 24 hours. **C,** Kaplan–Meier survival curves of PDX model mice (xenografted with patient #2 sample) treated with vehicle and purinostat mesylate (2.5 and 10 mg/kg), three times a week, respectively. The difference in survival between purinostat mesylate and vehicle groups is highly significant. **, $P < 0.01$ (Mantel–Cox test). WBC counts (**D**) and CD19$^+$ cell number (**E**) analysis in peripheral blood of PDX model mice after 7, 14, and 21 days of vehicle or purinostat mesylate treatments. The difference on day 21 between purinostat mesylate and vehicle groups is significant. *, $P < 0.05$ ($n = 3$, t test). **F,** Comparison of the size and weight of the spleens from vehicle or purinostat mesylate groups after 21-day treatment. **G,** Western blot analysis was done to analyze the protein levels of BCR-ABL, HSP90, p-SRC(Tyr416), c-MYC, HCK, Ac-H4, and Ac-H3 in spleens from vehicle or purinostat mesylate groups after 21 days treatment. GAPDH was used as loading control. Each point represents the mean value of 3 individual mice ± SD.

in the clinics and would achieve better therapeutic effects and less side effects.

Unlike other pan-HDAC inhibitors, purinostat mesylate is a highly selective inhibitor against class I and IIb with approximately 1,000-fold higher than class IIa and IV HDACs, which may explain its better safety profile. Compared with BL-2 secondary engraft mouse model, purinostat mesylate had no effect on acetylation of H3 and H4 in healthy mice (Supplementary Fig. S1B). In the 4-week toxicity study in 1 mg/kg purinostat mesylate group, at the end of recovery period, all beagle dogs survived in good condition with the normal clinical pathology parameters. Furthermore, in the *in vitro* hERG testing, no obvious inhibition was observed at the highest tested concentration of 100 μmol/L. In comparison, the IC_{50} of LBH589 in hERG inhibition was approximately 3.5 μmol/L (50). Compared with LBH589, purinostat mesylate has less toxicity and more selectivity.

In summary, purinostat mesylate displays potent efficacy both *in vitro* and *in vivo* on Ph^+ B-ALL, even associated with *BCR-ABL(T315I)* mutation and *IKZF1* exons deletion. Moreover, purinostat mesylate possesses the favorable pharmacokinetic and low toxicity characteristics. Collectively, preclinical assessment of the pharmacodynamics, pharmacokinetics, and toxicity of purinostat mesylate support it as a promising candidate drug for clinical studies in patients with Ph^+ B-ALL. Currently, purinostat mesylate has been approved by NMPA of China and this study will guide the design of purinostat mesylate clinical trials for Ph^+ B-ALL.

Disclosure of Potential Conflicts of Interest

No potential conflicts of interest were disclosed.

Authors' Contributions

Conception and design: Y. Hu, T. Niu, L. Chen
Development of methodology: L. Yang, Q. Qiu, M. Tang, F. Wang, D. Yi
Acquisition of data (provided animals, acquired and managed patients, provided facilities, etc.): L. Yang, Q. Qiu, M. Tang, Y. Yi, L. Chen
Analysis and interpretation of data (e.g., statistical analysis, biostatistics, computational analysis): L. Yang, Q. Qiu, M. Tang, Y. Yi, J. Yang, L. Chen
Writing, review, and/or revision of the manuscript: L. Yang, Q. Qiu, Y. Hu, T. Niu, L. Chen
Administrative, technical, or material support (i.e., reporting or organizing data, constructing databases): L. Yang, Q. Qiu, M. Tang, Z. Yang, Z. Zhu, S. Zheng, L. Zheng, Y. Chen, H. Ye, Y. Hu, L. Chen
Study supervision: Y. Hu, T. Niu, L. Chen
Other (conducted experiments): D. Yi, L. Zheng, L. Luo

Acknowledgments

The authors greatly appreciate the financial support from the Drug Innovation Major Project (2018ZX09711001-002-012), National Natural Science Foundation of China (81702991), and 1.3.5 Project for Disciplines of Excellence, West China Hospital, Sichuan University.

The costs of publication of this article were defrayed in part by the payment of page charges. This article must therefore be hereby marked *advertisement* in accordance with 18 U.S.C. Section 1734 solely to indicate this fact.

Received February 12, 2019; revised June 30, 2019; accepted August 13, 2019; published first August 22, 2019.

References

1. Bartram CR, de Klein A, Hagemeijer A, van Agthoven T, Geurts van Kessel A, Bootsma D, et al. Translocation of c-ab1 oncogene correlates with the presence of a Philadelphia chromosome in chronic myelocytic leukaemia. Nature 1983;306:277–80.
2. Peng C, Brain J, Hu Y, Goodrich A, Kong L, Grayzel D, et al. Inhibition of heat shock protein 90 prolongs survival of mice with BCR-ABL-T315I-induced leukemia and suppresses leukemic stem cells. Blood 2007;110:678–85.
3. Talpaz M, Shah NP, Kantarjian H, Donato N, Nicoll J, Paquette R, et al. Dasatinib in imatinib-resistant Philadelphia chromosome-positive leukemias. N Engl J Med 2006;354:2531–41.
4. Cony-Makhoul P, Gardembas M, Coiteux V, Carpentier N, Pommier C, Violet I, et al. Nilotinib after imatinib first-line: a real-life longitudinal cohort of patients with chronic myeloid leukaemia in chronic phase. Br J Haematol 2018;180:356–64.
5. Pavlovsky C, Chan O, Talati C, Pinilla-Ibarz J. Ponatinib in the treatment of chronic myeloid leukemia and philadelphia chromosome positive acute lymphoblastic leukemia. Future Oncol 2018;15:257–69.
6. Budhraja A, Turnis ME, Churchman ML, Kothari A, Yang X, Xu H, et al. Modulation of navitoclax sensitivity by dihydroartemisinin-mediated MCL-1 repression in BCR-ABL(+) B-lineage acute lymphoblastic leukemia. Clin Cancer Res 2017;23:7558–68.
7. Chen Y, Hu Y, Michaels S, Segal D, Brown D, Li S. Inhibitory effects of omacetaxine on leukemic stem cells and BCR-ABL-induced chronic myeloid leukemia and acute lymphoblastic leukemia in mice. Leukemia 2009;23:1446–54.
8. Seymour JF, Kim DW, Rubin E, Haregewoin A, Clark J, Watson P, et al. A phase 2 study of MK-0457 in patients with BCR-ABL T315I mutant chronic myelogenous leukemia and philadelphia chromosome-positive acute lymphoblastic leukemia. Blood Cancer J 2014;4:e238.
9. Hu Y, Swerdlow S, Duffy TM, Weinmann R, Lee FY, Li S. Targeting multiple kinase pathways in leukemic progenitors and stem cells is essential for improved treatment of Ph+ leukemia in mice. PNAS 2006;103:16870–5.
10. Nicolini FE, Mauro MJ, Martinelli G, Kim DW, Soverini S, Muller MC, et al. Epidemiologic study on survival of chronic myeloid leukemia and Ph(+) acute lymphoblastic leukemia patients with BCR-ABL T315I mutation. Blood 2009;114:5271–8.
11. Gupta P, Kathawala RJ, Wei L, Wang F, Wang X, Druker BJ, et al. PBA2, a novel inhibitor of imatinib-resistant BCR-ABL T315I mutation in chronic myeloid leukemia. Cancer Lett 2016;383:220–9.
12. Jabbour E, Kantarjian H, Ravandi F, Thomas D, Huang X, Faderl S, et al. Combination of hyper-CVAD with ponatinib as first-line therapy for patients with Philadelphia chromosome-positive acute lymphoblastic leukaemia: a single-centre, phase 2 study. Lancet Oncol 2015;16:1547–55.
13. Cortes JE, Kim DW, Pinilla-Ibarz J, le Coutre P, Paquette R, Chuah C, et al. A phase 2 trial of ponatinib in Philadelphia chromosome-positive leukemias. N Engl J Med 2013;369:1783–96.
14. Cortes JE, Kantarjian H, Shah NP, Bixby D, Mauro MJ, Flinn I, et al. Ponatinib in refractory Philadelphia chromosome-positive leukemias. N Engl J Med 2012;367:2075–88.
15. Zabriskie MS, Eide CA, Tantravahi SK, Vellore NA, Estrada J, Nicolini FE, et al. BCR-ABL1 compound mutations combining key kinase domain positions confer clinical resistance to ponatinib in Ph chromosome-positive leukemia. Cancer Cell 2014;26:428–42.
16. Maude SL, Laetsch TW, Buechner J, Rives S, Boyer M, Bittencourt H, et al. Tisagenlecleucel in children and young adults with B-cell lymphoblastic leukemia. N Engl J Med 2018;378:439–48.
17. Black KL, Naqvi AS, Asnani M, Hayer KE, Yang SY, Gillespie E, et al. Aberrant splicing in B-cell acute lymphoblastic leukemia. Nucleic Acids Res 2018;47:1043.
18. Sikaria S, Aldoss I, Akhtari M. Monoclonal antibodies and immune therapies for adult precursor B-acute lymphoblastic leukemia. Immunol Lett 2016;172:113–23.
19. Fischer J, Paret C, El Malki K, Alt F, Wingerter A, Neu MA, et al. CD19 Isoforms enabling resistance to CART-19 immunotherapy are expressed in B-ALL patients at initial diagnosis. J Immunother 2017;40:187–95.

20. Ruella M, Xu J, Barrett DM, Fraietta JA, Reich TJ, Ambrose DE, et al. Induction of resistance to chimeric antigen receptor T cell therapy by transduction of a single leukemic B cell. Nat Med 2018;24: 1499–503.
21. Prince HM, Bishton M, Harrison S. The potential of histone deacetylase inhibitors for the treatment of multiple myeloma. Leuk Lymphoma 2008; 49:385–7.
22. Vilas-Zornoza A, Agirre X, Abizanda G, Moreno C, Segura V, De Martino Rodriguez A, et al. Preclinical activity of LBH589 alone or in combination with chemotherapy in a xenogeneic mouse model of human acute lymphoblastic leukemia. Leukemia 2012;26: 1517–26.
23. Eckschlager T, Plch J, Stiborova M, Hrabeta J. Histone deacetylase inhibitors as anticancer drugs. Int J Mol Sci 2017;18. doi: 10.3390/ijms18071414.
24. Marks PA. The clinical development of histone deacetylase inhibitors as targeted anticancer drugs. Expert Opin Investig Drugs 2010;19: 1049–66.
25. Yan B, Chen Q, Shimada K, Tang M, Li H, Gurumurthy A, et al. Histone deacetylase inhibitor targets CD123/CD47-positive cells and reverse chemoresistance phenotype in acute myeloid leukemia. Leukemia 2018;33: 931–44.
26. Ding H, Peterson KL, Correia C, Koh B, Schneider PA, Nowakowski GS, et al. Histone deacetylase inhibitors interrupt HSP90*RASGRP1 and HSP90*CRAF interactions to upregulate BIM and circumvent drug resistance in lymphoma cells. Leukemia 2017;31:1593–602.
27. Sattler M, Griffin JD. Molecular mechanisms of transformation by the BCR-ABL oncogene. Semin Hematol 2003;40:4–10.
28. Danhauser-Riedl S, Warmuth M, Druker BJ, Emmerich B, Hallek M. Activation of Src kinases p53/56lyn and p59hck by p210bcr/abl in myeloid cells. Cancer Res 1996;56:3589–96.
29. Hu Y, Liu Y, Pelletier S, Buchdunger E, Warmuth M, Fabbro D, et al. Requirement of Src kinases Lyn, Hck and Fgr for BCR-ABL1-induced B-lymphoblastic leukemia but not chronic myeloid leukemia. Nat Genet 2004;36:453–61.
30. West AC, Johnstone RW. New and emerging HDAC inhibitors for cancer treatment. J Clin Invest 2014;124:30–9.
31. Lu X, Ning Z, Li Z, Cao H, Wang X. Development of chidamide for peripheral T-cell lymphoma, the first orphan drug approved in China. Intractable Rare Dis Res 2016;5:185–91.
32. Popat R, Brown SR, Flanagan L, Hall A, Gregory W, Kishore B, et al. Extended follow-up and the feasibility of panobinostat maintenance for patients with relapsed multiple myeloma treated with bortezomib, thalidomide, dexamethasone plus panobinostat (MUK six open label, multi-centre phase I/II clinical trial). Br J Haematol 2018;185:573–8.
33. Smolewski P, Robak T. The discovery and development of romidepsin for the treatment of T-cell lymphoma. Expert Opin Drug Discov 2017;12: 859–73.
34. Sivaraj D, Green MM, Gasparetto C. Panobinostat for the management of multiple myeloma. Future Oncol 2017;13:477–88.
35. Campbell P, Thomas CM. Belinostat for the treatment of relapsed or refractory peripheral T-cell lymphoma. J Oncol Pharm Pract 2017;23: 143–7.
36. Moskowitz AJ, Horwitz SM. Targeting histone deacetylases in T-cell lymphoma. Leuk Lymphoma 2017;58:1306–19.
37. Nebbioso A, Manzo F, Miceli M, Conte M, Manente L, Baldi A, et al. Selective class II HDAC inhibitors impair myogenesis by modulating the stability and activity of HDAC-MEF2 complexes. EMBO Rep 2009;10: 776–82.
38. Guedes-Dias P, Oliveira JM. Lysine deacetylases and mitochondrial dynamics in neurodegeneration. Biochim Biophys Acta 2013;1832: 1345–59.
39. Yanginlar C, Logie C. HDAC11 is a regulator of diverse immune functions. Biochim Biophys Acta Gene Regul Mech 2018;1861:54–9.
40. U.S. Food and Drug Administration Farydak [prescribing information]. Available from: https://www.accessdata.fda.gov/drugsatfda_docs/label/2015/205353s000lbl.pdf.
41. Chen Y, Wang X, Xiang W, He L, Tang M, Wang F, et al. Development of purine-based hydroxamic acid derivatives: potent histone deacetylase inhibitors with marked in vitro and in vivo antitumor activities. J Med Chem 2016;59:5488–504.
42. Wang F, Zheng L, Yi Y, Yang Z, Qiu Q, Wang X, et al. SKLB-23bb, a HDAC6-selective inhibitor, exhibits superior and broad-spectrum antitumor activity via additionally targeting microtubules. Mol Cancer Ther 2018;17: 763–75.
43. Atadja P. Development of the pan-DAC inhibitor panobinostat (LBH589): successes and challenges. Cancer Lett 2009;280:233–41.
44. Furumai R, Matsuyama A, Kobashi N, Lee KH, Nishiyama M, Nakajima H, et al. FK228 (depsipeptide) as a natural prodrug that inhibits class I histone deacetylases. Cancer Res 2002;62:4916–21.
45. Ning ZQ, Li ZB, Newman MJ, Shan S, Wang XH, Pan DS, et al. Chidamide (CS055/HBI-8000): a new histone deacetylase inhibitor of the benzamide class with antitumor activity and the ability to enhance immune cell-mediated tumor cell cytotoxicity. Cancer Chemother Pharmacol 2012;69: 901–9.
46. Daley GQ, Van Etten RA, Baltimore D. Induction of chronic myelogenous leukemia in mice by the P210bcr/abl gene of the Philadelphia chromosome. Science 1990;247:824–30.
47. Reavie L, Buckley SM, Loizou E, Takeishi S, Aranda-Orgilles B, Ndiaye-Lobry D, et al. Regulation of c-Myc ubiquitination controls chronic myelogenous leukemia initiation and progression. Cancer Cell 2013;23: 362–75.
48. Sillaber C, Gesbert F, Frank DA, Sattler M, Griffin JD. STAT5 activation contributes to growth and viability in Bcr/Abl-transformed cells. Blood 2000;95:2118–25.
49. Wu L, Yu J, Chen R, Liu Y, Lou L, Wu Y, et al. Dual inhibition of Bcr-Abl and Hsp90 by C086 potently inhibits the proliferation of imatinib-resistant CML cells. Clin Cancer Res 2015;21:833–43.
50. U.S. Food and Drug Administration. Center for Drug Evaluation and Research. Application Number: 205353Orig1s000. Pharmacology Review(s). Available from: https://www.accessdata.fda.gov/drugsatfda_docs/nda/2015/205353Orig1s000PharmR.pdf.